Actin-Binding Protein 1 Regulates B Cell Receptor-Mediated Antigen Processing and Presentation in Response to B Cell Receptor Activation[1]

Olusegun O. Onabajo[*], **Margaret K. Seeley**[*], **Amruta Kale**[*], **Britta Qualmann**[†], **Michael Kessels**[†], **Jin Han**[‡], **Tse-Hua Tan**[‡], and **Wenxia Song**[2],[*]

[*]Department of Cell Biology and Molecular Genetics, University of Maryland, College Park, MD 20742

[†]Leibniz Institute for Neurobiology, Magdeburg, Germany, and Friedrich-Schiller-University, Jena, Germany

[‡]Department of Microbiology and Immunology, Baylor College of Medicine, Houston, TX 77030

Abstract

The BCR serves as both signal transducer and Ag transporter. Binding of Ags to the BCR induces signaling cascades and Ag processing and presentation, two essential cellular events for B cell activation. BCR-initiated signaling increases BCR-mediated Ag-processing efficiency by increasing the rate and specificity of Ag transport. Previous studies showed a critical role for the actin cytoskeleton in these two processes. In this study, we found that actin-binding protein 1 (Abp1/HIP-55/SH3P7) functioned as an actin-binding adaptor protein, coupling BCR signaling and Ag-processing pathways with the actin cytoskeleton. Gene knockout of Abp1 and overexpression of the Src homology 3 domain of Abp1 inhibited BCR-mediated Ag internalization, consequently reducing the rate of Ag transport to processing compartments and the efficiency of BCR-mediated Ag processing and presentation. BCR activation induced tyrosine phosphorylation of Abp1 and translocation of both Abp1 and dynamin 2 from the cytoplasm to plasma membrane, where they colocalized with the BCR and cortical F-actin. Mutations of the two tyrosine phosphorylation sites of Abp1 and depolymerization of the actin cytoskeleton interfered with BCR-induced Abp1 recruitment to the plasma membrane. The inhibitory effect of a dynamin proline-rich domain deletion mutant on the recruitment of Abp1 to the plasma membrane, coimmunoprecipitation of dynamin with Abp1, and coprecipitation of Abp1 with GST fusion of the dyanmin proline-rich domain demonstrate the interaction of Abp1 with dynamin 2. These results demonstrate that the BCR regulates the function of Abp1 by inducing Abp1 phosphorylation and actin cytoskeleton rearrangement, and that Abp1 facilitates BCR-mediated Ag processing by simultaneously interacting with dynamin and the actin cytoskeleton. *The Journal of Immunology*, 2008, 180: 6685–6695.

The B cell-mediated Ab responses constitute one of the major components of the immune system. B cells are activated through two separate stages of signals, and the BCR plays an

2Address correspondence and reprint requests to Dr. Wenxia Song, Department of Cell Biology & Molecular Genetics, University of Maryland, College Park, MD 20742. wenxsong@umd.edu .

Disclosures
The authors have no financial conflict of interest.

essential role in the generation of both stages of signals. The binding of Ags to the BCR induces signaling cascades that provide the first stage signals for B cell activation (1,2). Subsequently, the BCR internalizes the Ags to the endosomal system, where the Ags are processed and loaded onto MHC class II molecules. The interaction between B and T cells in the context of antigenic peptide-MHC class II complexes triggers the second stage of signals. The induction of affinity maturation and the establishment of B cell memory require both stages of signals (3,4).

The BCR serves as both signal transducer and Ag transporter. Binding of the BCR to multivalent Ags not only induces signaling transduction, but also triggers rapid internalization of the BCR and accelerates targeting of the BCR to Ag-processing compartments (5,6). The BCR increases the Ag-processing and presentation efficiency of B cells by increasing the kinetics and specificity of Ag uptake and transport to Ag-processing compartments (5,6), allowing B cells to present an Ag even when the Ag is sparse. BCR signaling and Ag processing/presentation functions have been shown to be interrelated. BCR signaling blockage by tyrosine kinase inhibitors (7,8), mutations of the tyrosine phosphorylation sites in the Igα chain of the BCR (9–11), and loss of function mutants for Lyn or Syk (12–14) inhibit accelerated Ag transport and lower the Ag-presenting efficiency of B cells. We showed previously that cross-linking the BCR induced the recruitment of clathrin to the cell surface and BCR-containing vesicles and the tyrosine phosphorylation of clathrin in lipid rafts, both of which were required for BCR internalization (15). The exact mechanisms underlying the interaction of BCR signaling and Ag transport pathways have not been well studied.

The involvement of the actin cytoskeleton in BCR-mediated activation of B cells has long been suggested. Early studies showed that Ag binding induced the translocation of the BCR and tyrosine kinases Lyn and Syk to the detergent-insoluble cytoskeletal fractions (16–18), reorganization of the actin cytoskeleton (19–23), and transient increases in F-actin levels in B cells (24,25). Hao and August (25) recently showed that disruption of the actin cytoskeleton altered BCR-induced activation of the MAPK ERK and transcription factors serum response factor, NF-AT, and NF-κB. We previously demonstrated that the dynamic property of the actin cytoskeleton was required for signal-stimulated BCR internalization. BCR endocytosis is blocked at the pinching-off step during clathrin-coated vesicle formation in the absence of the functional actin cytoskeleton (24). Stoddart et al. (26) suggested an actin cytoskeleton-dependent and clathrin-independent BCR internalization pathway in DT40 chicken B cells. It has recently been reported that myosin II, an actin motor, is activated upon BCR engagement and facilitates BCR-driven Ag processing and presentation by interacting with MHC class II-invariant chain complexes (27). The findings that the actin cytoskeleton undergoes reorganization in response to BCR signaling and this reorganization is required for signal-induced BCR internalization suggest a role for the actin cytoskeleton in cross-talk between BCR signaling and Ag-processing pathways.

Actin-binding protein 1 (Abp1,[3] SH3P7, or HIP-55) is a multidomain protein that contains two independent F-actin-binding domains (ABDs), a proline-rich domain (PRD), and a Src homology 3 (SH3) domain (28–30). The SH3 domain of Abp1 is closely related to the SH3 domain of murine cortactin, an F-actin-binding protein and a substrate of Src kinase. Thus, Abp1 is able to simultaneously interact with the actin cytoskeleton and molecules of other pathways (30–33). Abp1 was first cloned from yeast (34) and named Abp1p. Its mammalian

---

[3]Abbreviations used in this paper: Abp1, actin-binding protein 1; ABD, F-actin-binding domain; AF, Alexa Fluor; EαRFP, MHC class II I-E α-chain peptide fused with red fluorescence protein; LAMP-1, lysosome-associated membrane protein 1; N-WASP, neural Wiskott-Aldrich syndrome protein; PRD, proline-rich domain; RFP, red fluorescence protein; SH3, Src homology 3; Tf, transferrin; wt, wild type.

homologue was cloned later by several different research groups (28–30). Abp1 was found to bind F-actin and be capable of directly (in yeast) (35) or indirectly (in mammal) (28,36) regulating the ability of the Arp2/3 complex to assemble branched actin filament networks. In yeast, Abp1p directly interacts with RVS167/amphiphysin, an endocytosis machinery protein, and was recruited to cortical actin patches partially coinciding with sites of endocytosis (37). In mammalian cells, Abp1 accumulates in lamellipodia in response to growth factors or the expression of dominant-active Rac1 (28) and is involved in transferrin (Tf) receptor endocytosis by a direct interaction with dynamin (33), a GTPase that drives the release of the nascent clathrin-coated vesicles (38). The role of Abp1 in Tf receptor internalization was further confirmed in Abp1-deficient embryonic fibroblasts (39) and in cells where Abp1 was knocked down by small interfering RNA (40). Recently established Abp1 knockout mice exhibited a moderate reduction in synaptic endocytosis and a dramatic defect in the reformation of fusion-competent vesicles in synapses of hippocampal neurons (39). Abp1 deficiency also caused abnormal structure and function of multiple organs, including the spleen, heart, and lung in both heterozygous and homozygous mice (39).

In lymphocytes, Ag engagement of the BCR or TCR induces tyrosine phosphorylation of Abp1, probably by Lyn, Syk, or ZAP70 (29,41). Abp1 was found to be recruited to the immunological synapse of T cells and bind to phosphorylated ZAP70 in response to TCR stimulation (42). RNA interference of Abp1 inhibited TCR-induced activation of hematopoietic progenitor kinase 1 and the MAPK JNK (30,41). T cells from Abp1 knockout mice showed similar TCR signaling defects (43). Although T and B cells appeared to develop normally, T cells in Abp1$^{-/-}$ mice exhibited reduced T cell proliferation and IL-2 secretion. These defects were accompanied by reduced T cell-dependent Ab responses (43). Although the role of Abp1 in B cells has not yet been examined, the data accumulated to date suggest a potential role for Abp1 in interaction with both Ag receptor signaling and Ag transport pathways.

In this study, we examined the relationship of Abp1 with BCR signaling and Ag-processing and presentation pathways. We demonstrate that the BCR regulates the function of Abp1 by inducing Abp1 phosphorylation and actin cytoskeleton rearrangement, and that Abp1 facilitates BCR-mediated Ag processing by interacting with dynamin and the actin cytoskeleton.

Materials and Methods

Mice, cells, and cell culture

B cell lymphoma A20 IIA1.6 cells (H-2^d, IgG2a$^+$, FcγRIIB$^-$) were cultured in DMEM supplemented with 10% FBS. C57BL6 mice that were 6 ~ 8 wk old were purchased from Taconic Farms. Abp1 knockout mice (Abp1$^{-/-}$) were generated and crossed into a C57BL/6 background, as previously described (43). To isolate splenic B cells, single-cell suspensions of splenocytes were subjected to density-gradient centrifugation (2300 × g) in Ficoll (Sigma-Aldrich) to obtain mononuclear cells, treated with anti-Thy1.2 mAb (BD Biosciences) and guinea pig complement (Rockland Immunobiochemicals) to remove T cells, and panned for 2 h to remove monocytes.

DNA constructs and transfection

The cDNA of *myc*-tagged full-length (*myc*-Abp1), ABDs, PRD-SH3 domains (PRD-SH3), and SH3 domain of Abp1 were cloned into a pRK5 plasmid, as previously described (28). Mutations of tyrosines 337 and 347 to phenylalanines (*myc*-Abp1 Y337FY347F) were generated using the Stratagene quick change site-directed mutagenesis kit (Stratagene) and

confirmed by sequencing. DNA constructs were introduced into A20 B cells by electroporation using a Nucleofection kit (Amaxa).

Analysis of the movement of the BCR from the cell surface to late endosomes

B cells were incubated with Alexa Fluor (AF) 488-conjugated F(ab′)$_2$ goat anti-mouse IgG or IgM (Invitrogen) for 20 min at 4°C to label the surface BCR. Cells were washed and adhered to poly(lysine)-coated slides (Sigma-Aldrich) for 40 min at 4°C and then chased at 37°C for varying lengths of time to allow for BCR internalization. At the end of each time point, cells were fixed with 4% paraformaldehyde, permeabilized with 0.05% saponin, and incubated with a mAb specific for lysosome-associated membrane protein 1 (LAMP-1) (ID4B; American Type Culture Collection) and an AF633-conjugated secondary Ab. Myc-Abp1 was detected using Cy3 anti-c-*myc* mAb (Sigma-Aldrich). Endogenous Abp1 was detected using rabbit anti-Abp1 Ab (33) and an AF546-conjugated secondary Ab (Invitrogen). Cells were mounted with Biomedia gel mount (Electron Microscopy Sciences) and analyzed using a laser-scanning confocal fluorescence microscope (LSM 510; Zeiss). For quantitative analysis of images, the cellular distribution of the BCR was divided into three different categories, as follows: the BCR mainly distributed on the cell surface without colocalization with LAMP-1, extensively colocalized, and partially colocalized with LAMP-1 at the perinuclear region of cells. Cells were categorized by visual inspection. Over 100 cells from three independent experiments were analyzed for each time point, and the data were plotted as percentages of the total number of cells in the images. To quantify the levels of colocalization between the BCR and LAMP-1, the correlation coefficients of the staining for the BCR and LAMP-1 in individual cells were determined using the LSM510 software.

Analysis of BCR internalization

Splenic B cells were incubated with biotinylated F(ab′)$_2$ of goat anti-mouse IgM (20 µg/ml; Jackson ImmunoResearch Laboratories) for 30 min at 4°C to label the surface BCR. After washing off unbound Abs, cells were chased at 37°C for 0, 2, 5, and 20 min. The chase was terminated by adding ice-cold DMEM containing 6 mg/ml BSA. The biotinylated Abs remaining on the cell surface were stained with PE-streptavidin (5 µg/ml; Qiagen) at 4°C. The cells were then fixed and analyzed using a flow cytometer (FACS-Calibur; BD Biosciences). The data were plotted as a percentage of the mean fluorescence intensity of cell surface PE-streptavidin at time 0. To depolymerize the actin cytoskeleton, cells were treated with 5 µM latrunculin (Calbiochem) for 30 min at 37°C before the internalization assay, and latrunculin was also included in the incubation medium during the internalization assay.

Ag presentation assay

Splenic B cells were incubated sequentially with the following Abs and reagents at 4°C. Anti-CD32/CD16 mAb (BD Biosciences) was used to block FcγII/IIIRs. A peptide (aa 52–68) of MHC class II I-E α-chain fused with red fluorescence protein (EαRFP) was used as the Ag (a gift from M. Jenkins, University of Minnesota, Mineapolis, MN). An equivalent concentration of rabbit anti-red fluorescence protein (RFP; Rockland Immunochemicals) was used to bind to RFP and rabbit anti-mouse IgM (5 µg/ ml; Jackson ImmunoResearch Laboratories) to cross-link the BCR. Goat anti-rabbit IgG (Fc specific; 5 µg/ml; Jackson ImmunoResearch Laboratories) was used to target the EαRFP anti-RFP Ab complex to the BCR. B cells were allowed to internalize the Ag-Ab complex for 10 min at 37°C, washed, and incubated at 37°C for 14 h. After washing, cells were incubated with anti-CD32/CD16 mAb and biotin-conjugated mAb Y-Ae (eBioscience), followed by PE-streptavidin to label Eα-I-A^b complexes (44,45). Cells were fixed and analyzed using a flow cytometer. The surface expression level of MHC class II was monitored before and after the incubation with

the Ag-Ab complex using PE anti-mouse MHC class II (Miltenyi Biotec) by flow cytometry.

Analysis of cellular distributions of Abp1, F-actin, and dynamin 2

A20 B cells and splenic B cells were incubated with Cy5-conjugated Fab of rabbit anti-mouse IgG + M to label the BCR and activated by $F(ab')_2$ donkey anti-mouse IgG + M (20 µg/ml; Jackson ImmunoResearch Laboratories). Cells were permeabilized and stained with goat anti-Abp1 Ab for endogenous Abp1, Cy3 anti-*myc* Ab for transfected Abp1, antidynamin 2 Ab (BD Biosciences), or AF488-phalloidin (Invitrogen) for F-actin. Goat anti-mouse Abp1 Ab was generated by immunization of a goat with GST-Abp1 fusion proteins by Alpha Diagnostics International and purified using protein G-Sepharose column. To disrupt the actin cytoskeleton, cells were pretreated with 5 µM latrunculin for 30 min at 37°C. Cells were analyzed using a confocal fluorescence microscope. The recruitment of Abp1 to the cell surface was quantified by visually inspecting five randomly selected fields (~100 cells) from each of three independent experiments. Correlation coefficients between the staining of Abp1 and BCR in individual cells were determined using the LSM510 software to quantify the extent of the colocalization. Over 100 cells from two or three independent experiments were analyzed for each time point.

To further analyze the cellular distribution of Abp1 in relation to dynamin 2, A20 cells were cotransfected with *myc*-Abp1 and either GFP-dynamin 2 (GFP-Dyn) or GFP-dynamin 2 with its PRD deleted (GFP-ΔPRD) (gifts from M. McNiven, Mayo Clinic, Rochester, MN). The BCR was labeled using AF633-Fab goat anti-mouse IgG for 15 min at room temperature on poly(lysine)-coated slides. The cells were then activated with rabbit anti-mouse IgG (20 µg/ml) for 5 and 30 min at 37°C, followed by fixation and permeabilization. Transfected Abp1 was stained with Cy3 anti-*myc* Ab, and cells were analyzed using a confocal fluorescence microscope. Correlation coefficients between the staining of Abp1 and GFP-Dyn at the cell surface area were determined using the LSM510 software. Over 30 cells from three independent experiments were analyzed for each condition.

Analysis of tyrosine phosphorylation of Abp1

Untransfected A20 cells and A20 cells transfected with *myc*-Abp1 were activated by cross-linking the BCR with goat anti-mouse IgG (20 µg/ml) for indicated times and lysed in a lysis buffer containing 0.5% Triton X-100, 20 mM Tris-HCl (pH 7.5), 150 mM NaCl, 1 mM $MgCl_2$, 1 mM EGTA, 1 mM Na_3VO_4, and protease inhibitors (Sigma-Aldrich). Lysates were subjected to immunoprecipitation using rabbit anti-Abp1 Ab for endogenous Abp1 and anti-*myc* mAb (Bethyl Laboratories) for transfected Abp1. The immunoprecipitates were analyzed by SDS-PAGE and Western blotting, probing with anti-phosphotyrosine mAb (4G10; Upstate Biotechnology). The blots were stripped and reblotted with guinea pig anti-Abp1 (28) or anti-*myc* Abs.

Coimmunoprecipitation and coprecipitation of Abp1 and dynamin 2

A20 cells were activated with rabbit anti-mouse IgG for indicated times at 37°C and lysed with the 0.5% Triton X-100 lysis buffer. The lysates were subjected to immunoprecipitation using goat anti-Abp1 Ab and protein G-Sepharose beads, and the immunoprecipitates were analyzed using SDS-PAGE and Western blotting. The presence of dynamin 2 in the anti-Abp1 immunoprecipitates was detected using anti-dynamin 2 Ab (BD Biosciences), and Abp1 was detected using guinea pig anti-Abp1 Ab.

The DNA construct of GST-dynamin PRD fusion protein (GST-dynamin PRD; a gift from M. McNiven, Mayo Clinic, Rochester, MN) was expressed in the *Escherichia coli* BL21 strain. The bacteria were grown at 37°C in LB medium supplemented with 100 µg/ml

ampicillin until $OD_{600} = 1.0$. The synthesis of the fusion protein was induced by 1.0 mM isopropyl β-ᴅ-thiogalactoside (US Biological) for 3 h. Cells were harvested, washed, and lysed using a lysis buffer (140 mM NaCl, 2.7 mM KCl, 10 mM Na_2HPO_4, 1.8 mM KH_2PO_4 (pH 7.4), 1 mg/ml lysozyme, and protease inhibitor mixture) and three freeze-thaw cycles. The lysate was centrifuged at $70,000 \times g$ for 25 min at 4°C, and supernatant was loaded onto a GSTrap FF column (GE Healthcare). The column was washed with PBS and stored in PBS containing 0.05% sodium azide. A20 cells transfected with either *myc*-Abp1 or *myc*-Abp1-ABDs were activated with goat anti-mouse IgG (20 µg/ml) for indicated times at 37°C and lysed with the Triton X-100 lysis buffer. The lysates were incubated with GST-dynamin PRD beads overnight, and the precipitates were analyzed using SDS-PAGE and Western blotting. The presence of *myc*-Abp1 in the precipitates was detected using anti-*myc* mAb (BD Biosciences) and a HRP-conjugated secondary Ab.

Results

Abp1 is required for BCR-mediated Ag uptake

To test whether Abp1 plays a role in BCR-mediated Ag transport, the functions of Abp1 were disrupted by gene knockout and over-expression of dominant-negative mutants. The Abp1 knockout mouse model was previously developed by Han et al. (43), and the deletion of the Abp1 gene (Fig. 1*A* , *top panel*) and the absence of Abp1 protein expression (Fig. 1*A* , *bottom panel*) were confirmed by PCR analyses of genomic DNA and Western blot analyses of splenic B cell lysates. The movement of the BCR from the cell surface to the LAMP-1$^+$ compartment was followed by immunofluorescence microscopy (Fig. 1*B*). Based on the cellular distribution pattern of the BCR and LAMP-1, cells were categorized into three groups, as follows: 1) BCR colocalizing with LAMP-1 extensively in the perinuclear region; 2) BCR remaining on the cell surface and periphery with no significant colocalization with LAMP-1; and 3) BCR partially colocalizing with LAMP-1. The numbers of cells in these three categories were plotted as percentages of the total number of cells in the field (Fig. 1*C*). After a 30-min chase at 37°C, the surface-labeled BCR was extensively colocalized with the LAMP-1 in over 60% of wild-type (wt) splenic B cells, compared with just ~30% of Abp1$^{-/-}$ splenic B cells (Fig. 1, *B* and *C*). In >60% of Abp1$^{-/-}$ splenic B cells, the BCR remained at the cell surface and periphery after a 30-min chase (Fig. 1, *B* and *C*), indicating that Abp1 deficiency dramatically slowed BCR-mediated Ag transport. This is further supported by the quantitative analysis of colocalization between the BCR and LAMP-1 staining. Although BCR cross-linking increased the correlation coefficients between the BCR and LAMP-1 in both wt and Abp1$^{-/-}$ splenic B cells, the increase in wt B cells was significantly greater than that in Abp1$^{-/-}$ B cells (Fig. 1*D*). To analyze the effect of Abp1 deficiency on the kinetics of BCR internalization, the surface BCR of splenic B cells from both wt and Abp1$^{-/-}$ mice were labeled with biotin F(ab′)$_2$ anti-mouse IgM at 4°C and chased for 0, 2, 5, and 20 min at 37°C. Biotin anti-mouse IgM remaining at the cell surface after the chase was detected with PE-streptavidin and quantified using flow cytometry. As shown in Fig. 1*E* , Abp1 deficiency significantly decreased the kinetics of BCR internalization. Furthermore, Abp1 deficiency and F-actin depolymerization by latrunculin treatment inhibited BCR internalization to a similar extent. These data demonstrate that Abp1 deficiency inhibits BCR-mediated Ag uptake, consequently reducing the rate of Ag transport to the Ag-processing compartment.

To determine which domain of Abp1 is important for BCR-mediated Ag transport, we introduced *myc*-tagged full-length Abp1 (*myc*-Abp1), two ABDs, *myc*-Abp1 with two tyrosine phosphorylation sites mutated (Y337F/Y347F), PRD and SH3 domains (PRD-SH3), or SH3 domain (SH3) of Abp1 (33) into A20 B cells by transient transfection. The movement of the BCR from the cell surface to late endosomes was analyzed using immunofluorescence microscopy. After 30-min chase, the BCR in >50% of cells that

underwent electroporation, but did not express transfected proteins, colocalized with LAMP-1 extensively in the perinuclear location (Fig. 2). Overexpression of full-length *myc*-Abp1, *myc*-Abp1 ABDs, or *myc*-Abp1 Y337FY347F did not alter the extent of the colocalization between the BCR and LAMP-1 (Fig. 2, *Aa–Al* and *B*), indicating that they had no significant effect on the movement of the BCR to the LAMP-1$^+$ compartment. In contrast, only 10–20% of cells that expressed *myc*-Abp1 PRD-SH3 or *myc*-Abp1 SH3 showed colocalization of the BCR with LAMP-1, and in ~70% of those cells, the BCR remained on the cell surface and periphery, displaying no significant colocalization with LAMP-1 after the 30-min chase (Fig. 2, *Am–At* and *B*). This indicates that overexpression of the SH3 domain of Abp1 inhibits the movement of the BCR from the cell surface into late endosomes and suggests a role for the SH3 domain of Abp1 in BCR-mediated Ag transport.

B cells with Abp1 deficiency are defective in BCR-mediated Ag presentation

The inhibitory effect of Abp1 deficiency on BCR internalization and transport to late endosomes suggests a reduced efficiency of Ag processing and presentation in Abp1$^{-/-}$ splenic B cells. To test this hypothesis, we determined the Ag-processing and presentation efficiency of mouse splenic B cells using an Eα peptide (aa 52– 68)-RFP (EαRFP) chimera as the Ag. To follow BCR-mediated Ag processing and presentation, we targeted EαRFP to the BCR using an Ab complex. The specific internalization and delivery of EαRFP by the BCR to late endosomes were confirmed by flow cytometry and immunofluorescence microscopy, respectively (data not shown). Eα peptide-loaded MHC class II I–A^b complexes (Eα-I-A^b) were detected using Y-Ae mAb (45,46), indicating levels of Ag presentation. Splenic B cells were incubated with different concentrations of EαRFP alone for pinocytosis-mediated Ag processing or EαRFP plus the Ab complex for BCR-mediated Ag processing at 37°C for 10 min to allow Ag internalization, and then washed and incubated at 37°C for 14 h. The surface Eα-I-A^b-staining levels were quantified by flow cytometry. The surface Eα-I-A^b level of wt splenic B cells incubated with the Ag-Ab complex was significantly higher than those incubated with EαRFP alone (Fig. 3, *A* and *B*), indicating a higher efficiency of BCR-mediated Ag processing and presentation than that of nonspecific mechanisms. In addition, the level of surface Eα-I-A^b on wt splenic B cells that were incubated with the Ag-Ab complex increased with the concentration of the complex (Fig. 3*B*). In comparison with wt splenic B cells, the surface Eα-I-A^b level in Abp1$^{-/-}$ B cells was significantly lower and did not increase with the concentration of the Ag-Ab complex (Fig. 3, *A* and *B*). BCR cross-linking increased the surface levels of MHC class II in both wt and Abp1$^{-/-}$ splenic B cells, and Abp1$^{-/-}$ B cells showed MHC class II expression levels similar to wt B cells before and after BCR cross-linking by the Ag-Ab complex (Fig. 3*C*). These results indicate that the decrease in surface Eα-I-A^b levels was not the result of decreased I-A^b expression. These data indicate that Abp1 deficiency decreases the efficiency of BCR-mediated Ag processing and presentation.

BCR activation induces recruitment of Abp1 to the plasma membrane and the internalizing BCR

To examine the relationship of Abp1 with BCR signaling pathway, we analyzed the cellular redistribution of Abp1 in response to BCR activation in both A20 and splenic B cells using immunofluorescence microscopy. B cells were activated via incubation with cross-linking Ab for 2 and 10 min at 37°C, fixed, permeabilized, and labeled with an Ab specific for Abp1. In the absence of BCR cross-linking, Abp1 was primarily located in the cytoplasm (Fig. 4, *Aa*, *Ab*, and *Ca*). BCR cross-linking for 2 min led to a redistribution of Abp1 to the cell surface (Fig. 4, *Af*, *Ag*, and *Ce*). Nearly 55% of the A20 B cells showed this redistribution after 2 min of activation, compared with only 10% of the unstimulated cells (Fig. 4*B*). By 10 min, Abp1 began returning to the cytoplasm (Fig. 4, *Ak*, *Al*, and *Ci*). Such redistribution from the cytoplasm to plasma membrane in response to BCR activation was

observed with both transfected *myc*-Abp1 and endogenous Abp1 in A20 and splenic B cells (Fig. 4, *A–C*), showing that transfected *myc*-Abp1 behaved in a similar manner to the endogenous Abp1.

To examine the cellular distribution of Abp1 relative to the Ag-bound BCR, the surface BCR in both A20 and splenic B cells was labeled and cross-linked at 4°C, and the cells were warmed up to 37°C for 2 and 10 min. After fixation and permeabilization, *myc*-Abp1 and endogenous Abp1 were labeled with anti-*myc* mAb and anti-Abp1 Ab, respectively. Before the cells were warmed to 37°C, Abp1 was primarily localized in the cytoplasm, and there was little colocalization of the cytoplasmic Abp1 with the surface BCR observed (Fig. 4, *Ab–Ae* and *Ca–Cd*). After 2-min incubation at 37°C, we observed a dramatic increase in the colocalization of Abp1 with the BCR at the cell surface (Fig. 4, *Ag–Aj* and *Ce–Ch*), suggesting that Abp1 was recruited to the surface BCR in response to the stimulation. By 10 min, when some of the BCR had been internalized and moved to late endosomes, Abp1 began moving back to the cytoplasm; however, some remained colocalized with the intracellular BCR (Fig. 4, *Al–Ao* and *Ci–Cl*). The correlation analysis of splenic B cells showed an increase in the colocalization of Abp1 with the BCR at 2 min after BCR cross-linking, and this colocalization declined at later time points (Fig. 4*D*). These results showed that BCR stimulation induced the recruitment of Abp1 to the surface and internalizing BCR.

BCR-induced redistribution of Abp1 depends on BCR-induced tyrosine phosphorylation of Abp1

Abp1 has been reported to undergo tyrosine phosphorylation at Y337 and Y347 in response to BCR stimulation (29). To test whether BCR-induced tyrosine phosphorylation of Abp1 is related to its cellular distribution, we followed the time course of the tyrosine phosphorylation of endogenous Abp1 and transfected *myc*-Abp1. Untransfected A20 B cells and A20 B cells that were transfected with full-length *myc*-Abp1 were activated for indicated times by cross-linking the BCR. Cells were lysed, and the cell lysates were subjected to immunoprecipitation using anti-Abp1 Ab for endogenous Abp1 or anti-*myc* mAb for transfected *myc*-Abp1. The immunoprecipitates were analyzed by SDS-PAGE and Western blot, probing for phosphotyrosine. As shown in Fig. 5*A* , cross-linking of the BCR increased the tyrosine phosphorylation of endogenous Abp1 as early as 2 min, and this increase appeared to be sustained at least for 30 min (Fig. 5*A* , *top panels*). Similarly, BCR cross-linking induced the tyrosine phosphorylation of *myc*-Abp1. This phosphorylation peaked at 2 min, but rapidly decreased to undetectable levels by 10 min (Fig. 5*A* , *bottom panels*). These results show that BCR cross-linking increases tyrosine phosphorylation of Abp1 at a time corresponding to BCR-induced redistribution of Abp1.

To test whether BCR-induced tyrosine phosphorylation of Abp1 is important for its cellular redistribution, we determined the effect of mutations of Abp1 tyrosines 337 and 347 into phenylalanines (Abp1 Y337F/Y347F) on the cellular redistribution of Abp1. The DNA construct of *myc*-Abp1 Y337F/Y347F was introduced into A20 B cells by transfection, and its cellular redistribution was analyzed by immunofluorescence microscopy in comparison with wt *myc*-Abp1 (Fig. 5*B*, *a–d*). The percentage of wt *myc*-Abp1-expressing cells showing cell surface redistribution of Abp1 increased from 20 to 80% after BCR cross-linking for 2 min (Fig. 5, *Ba*, *Bb*, and *C*). In contrast, there was no significant increase in the percentage of Abp1 Y337F/Y347F-expressing cells showing the redistribution (Fig. 5, *Bc*, *Bd*, and *C*). This indicates that the Abp1 redistribution depends on BCR-induced tyrosine phosphorylation of Abp1.

BCR-induced Abp1 redistribution depends on the actin cytoskeleton

BCR activation induces reorganization of the actin cytoskeleton (24,25). The presence of two ABDs in Abp1 implies that its cellular redistribution may rely on BCR-induced actin cytoskeleton reorganization. To test this hypothesis, we analyzed the cellular distribution of Abp1 relative to F-actin and tested the effect of a G-actin sequestering agent latrunculin B on BCR-induced redistribution of Abp1. In A20 B cells, *myc*-Abp1 was colocalized with F-actin extensively with and without BCR activation (Fig. 6*A*). Both F-actin and endogenous Abp1 were located at the cell periphery and cytoplasm in unstimulated cells (Fig. 6, *A* and *Ba*) and rapidly moved to the plasma membrane upon BCR activation (Fig. 6, *A* and *Bc*). In latrunculin-treated cells, Abp1 was primarily located in the cytoplasm with (Fig. 6*Bd*) or without BCR activation (Fig. 6*Bb*). Latrunculin B treatment significantly decreased the number of cells showing BCR-induced redistribution of Abp1 (Fig. 6, *B* and *C*). These data indicate that BCR-induced Abp1 redistribution is dependent on the actin cytoskeleton.

The interaction of Abp1 with dynamin 2

The interaction of dynamin and Abp1 through their PRD and SH3 domains has been shown to be important for Tf internalization (33). To examine the relationship between Abp1 and dynamin 2 in B cells, we followed the interaction of these two proteins by immunofluorescence microscopy, coimmunoprecipitation, and coprecipitation. Immunofluorescence microscopy studies showed that similar to Abp1, dynamin 2 was primarily distributed in the cytoplasm in the absence of stimulation. In response to BCR cross-linking, dynamin 2 was recruited from the cytoplasm to plasma membrane, where it colocalized with Abp1 (Fig. 7*A*). The core-cruitment of dynamin 2 with Abp1 upon BCR activation suggests a potential interaction between Abp1 and dynamin 2. To further test whether the interaction between the two proteins depends on their SH3 and PRD, we cotransfected A20 B cells with *myc*-Abp1 and GFP-dynamin 2 (GFP-Dyn; Fig. 7*B, a–l*) or GFP-Dyn with its PRD deleted (GFP-ΔPRD; Fig. 7*B, m–x*) and followed the cellular distribution of these proteins by immunofluorescence microscopy. Similar to endogenous dynamin 2, GFP-Dyn showed a cytoplamic distribution in the absence of stimulation (Fig. 7*Bc*) and was recruited to the cell surface, where it colocalizes with *myc*-Abp1 and the BCR after cross-linking of the BCR for 5 min (Fig. 7*B, e–h*). By 30 min, both proteins accumulated in the perinuclear region with the BCR (Fig. 7*B, i–l*). In cells coexpressing *myc*-Abp1 and GFP-ΔPRD, both proteins appeared to be in the cytoplasm without BCR activation (Fig. 7*B, m–p*). Upon BCR cross-linking, both GFP-ΔPRD and Abp1 showed punctate staining patterns (Fig. 7*B, r–t* and *v–x*). In contrast to what was observed in cells coexpressing GFP-Dyn and *myc*-Abp1, GFP-ΔPRD and Abp1 were neither recruited to the cell surface, nor colocalized with each other (Fig. 7*B, q–x*). The correlation analysis further showed that the colocalization coefficients between GFP-Dyn and *myc*-Abp1 were increased in response to BCR activation (Fig. 7*C*). In contrast, there was no significant increase in the colocalization coefficients between GFP-ΔPRD and *myc*-Abp1 following BCR activation (Fig. 7*C*). These results suggest that dynamin 2 interacts with Abp1 through its PRD.

We further examined the interaction between dynamin 2 and Abp1 using coimmunoprecipitation and GST-fusion protein coprecipitation. The cell lysates from unstimulated and stimulated A20 B cells were subjected to immunoprecipitation using a polyclonal Ab specific for Abp1. The presence of dynamin 2 in the Abp1 immunoprecipitates was detected by a dynamin 2-specific Ab. As shown in Fig. 7*D* , dynamin 2 was detected in the Abp1 immunoprecipitates in the presence or absence of BCR activation, and dynamin 2 was absent only when anti-Abp1 Ab was omitted. This result indicates a constitutive interaction between dynamin 2 and Abp1. To further confirm whether this interaction is mediated through the PRD of dynamin 2 and the SH3 domain of Abp1, we used a GST fusion protein of dynamin 2 PRD (GST-Dyn-PRD) to precipitate

Abp1 from the lysates of cells expressing full-length *myc*-Abp1 and *myc*-Abp1 ABDs. Similar to the coimmunoprecipitation of endogenous dynamin 2 with Abp1, GST-Dyn-PRD coprecipitated similar amounts of *myc*-Abp1 from the lysate of A20 cells that were treated or untreated with BCR cross-linking Abs (Fig. 7*E*), confirming the constitutive interaction of dynamin 2 with Abp1. In contrast, GST-dynamin-PRD failed to precipitate *myc*-Abp1 ABDs (Fig. 7*E*), indicating the PRD and SH3 domains of dynamin and Abp1 are essential for their interaction. These results further confirm that Abp1 and dynamin 2 constitutively interact with each other through their SH3 and PRD.

Discussion

This study revealed a critical role for Abp1 in BCR-mediated Ag processing and presentation. Abp1 gene knockout and overexpression of the Abp1 SH3 domain reduced the rates of BCR-mediated Ag uptake, consequently reducing the rate of Ag transport to the Ag-processing compartment and the efficiency of Ag processing and presentation. B cells process and present Ags to acquire T cell help, which is essential for the induction of isotype switching, somatic hypermutation, and affinity maturation in B cells. The BCR increases B cell Ag processing and presentation efficiency by binding to Ags with high specificity and affinity and by initiating rapid internalization and transport of Ags to Ag-processing compartments. This allows B cells to present specific Ags even when Ag concentrations are extremely low. A previous study showed defective Ab responses to T cell-dependent Ags and reduced TCR-mediated signaling and T cell activation in Abp1$^{-/-}$ mice (43). In this study, we discovered defects in Ag processing and presentation of Abp1$^{-/-}$ B cells. Lowering the efficiency of B cells to process and present Ags to T cells would decrease the sensitivity of T cell-dependent B cell activation, contributing to defective T cell-dependent Ab responses in Abp1$^{-/-}$ mice.

Abp1 contains two independent ABDs in the N terminus, and a SH3 domain and a PRD or flexible domain in its C terminus (28–30). Its multiple protein-protein-interacting domains enable Abp1 to interconnect different cellular apparatuses. Previous studies implicate Abp1 as an actin adaptor protein connecting the actin cytoskeleton to endocytosis machinery. The null mutation of the yeast homologue of Abp1, Abp1p, resulted in defects similar to those seen in Rvs167/amphiphysin mutation, including sporulation and reduced viability under certain suboptimal growth conditions. Double mutations in ABP1 and RVS167/amphiphysin genes or one of the genes encoding other cytoskeletal components were genetic lethal (47). In mammalian cells, Abp1 has been shown to be essential for Tf internalization (33,40) and synaptic vesicle recycling (39). In this study, we showed that Abp1 was required for efficient BCR-mediated Ag internalization, further demonstrating an essential role for Abp1 in endocytosis. Previous studies have shown that Abp1 interacts directly with proteins of the endocytic machinery, including rvs167/amphiphysin in yeast (47) and dynamin in mammalian cells (33). Both amphiphysin and dynamin are important for the membrane fission step of endocytosis (38,48). Furthermore, Abp1p was recruited to the endocytosis sites along with Arp2/3 and actin in yeast (37), suggesting a role for Abp1 in endocytic vesicle formation from the plasma membrane. However, a recent study using Abp1$^{-/-}$ mice placed Abp1 function downstream of vesicle fission in synaptic vesicle recycling in hippocampal neurons (39). Our previous studies showed that the dynamic properties of the actin cytoskeleton were required for BCR internalization at the fission step of clathrin-coated vesicle formation (24). In this study, we found that Abp1 deficiency and actin depolymerization inhibited BCR internalization to a similar extent. Furthermore, Abp1, F-actin, and dynamin 2 were recruited to the BCR at the plasma membrane at the same time and appear to interact with each other. These findings further support a role for Abp1 in clathrin-coated vesicle fission.

Unlike the constitutive internalization of Tf receptor, BCR internalization is triggered by Ag binding and dependent on BCR-mediated signaling (5–8). Previously, we showed that BCR activation induced the recruitment of clathrin to the BCR and phosphorylation of clathrin within lipid rafts, both of which were required for BCR internalization (26). In this study, we found that BCR activation induced the recruitment of Abp1 to the plasma membrane and to the internalizing BCR, suggesting that BCR signaling regulates the function of Abp1. Indeed, our data revealed that BCR activation induced tyrosine phosphorylation of Abp1, and that this phosphorylation was required for the recruitment of Abp1 to the cell surface and BCR. Abp1 colocalized with cortical F-actin, and BCR-induced recruitment of Abp1 to the cell surface depended on the actin cytoskeleton. These data indicate that BCR signaling can regulate the subcellular location of Abp1 through the tyrosine phosphorylation of Abp1 and the reorganization of the actin cytoskeleton. This is in line with a previous study showing the translocation of Abp1 from the perinuclear region to the leading edge of cells in a pattern that overlaps with Arp2/3 complex localization in response to activation of the GTPase Rac (28). The finding of a synchronized cellular reorganization of the actin cytoskeleton, Abp1, and dynamin 2 in response to BCR stimulation suggests that BCR signaling regulates the interaction of Abp1 with the actin cytoskeleton and dynamin 2. The interaction of Abp1 with dynamin during clathrin-mediated endocytosis has been previously reported (33). In this study, we demonstrate this interaction in B cells by coimmunoprecipitation and GST fusion protein co-precipitation. Although the interaction between Abp1 and dynamin 2 appeared to be constitutive, our observation of corecruitment of Abp1 and dynamin 2 to the plasma membrane following BCR activation indicates that BCR signaling regulates the subcellular location where Abp1 and dynamin 2 interact.

Another possible mechanism through which Abp1 functions in endocytosis is by regulating the dynamics of the actin cytoskeleton. In yeast, Abp1p recruits Arp2/3 complexes to the sites of actin filaments and is required for Arp2/3 complex activation in vitro (35). Overexpression of Abp1p in yeast causes severe defects in cellular actin organization (34). Pinyol et al. (36) recently showed that Abp1 directly interacted with neural Wiskott-Aldrich syndrome protein (N-WASP), an activator of Arp 2/3 complex, and activated N-WASP in cooperation with Cdc42, suggesting that Abp1 may regulate the actin cytoskeleton indirectly through N-WASP. However, obvious defects in the actin cytoskeleton have not been observed in Abp1$^{-/-}$ B cells and B cells overexpressing Abp1 and its dominant-negative mutants (data not shown).

Abp1 has been shown to serve as a signaling regulator in T cells. Abp1 is recruited to the immunological synapse formed between T cells and APCs (42) and regulates the distal signaling of the TCR, including the activation of hematopoietic progenitor kinase 1, the MAPK JNK, and the transcription factor NF-AT (30,41,43). It is possible that Abp1 plays a similar role in regulation of BCR signaling events, which may provide feedback signals from the actin cytoskeleton and endocytic machinery to BCR-mediated signaling pathway.

This study demonstrates the role of Abp1 in coupling BCR signaling and Ag-processing/presentation functions by interacting with BCR signaling, endocytic, and actin cytoskeletal apparatuses. BCR activation induced Abp1 tyrosine phosphorylation and actin cytoskeleton reorganization, both of which are required for the recruitment of Abp1 to BCR internalization sites. Upon being recruited to the plasma membrane, the interaction of Abp1 with the actin cytoskeleton and endocytic proteins, like dynamin 2, drives BCR internalization. Future studies will further examine the molecular mechanisms for interactions of Abp1 with BCR signaling, endocytic, and actin cytoskeletal apparatuses and regulatory mechanisms for these interactions.

Acknowledgments

References

1. Kurosaki T. Genetic analysis of B cell antigen receptor signaling. Annu. Rev. Immunol 1999;17:555–592. [PubMed: 10358768]

2. Dal Porto JM, Gauld SB, Merrell KT, Mills D, Pugh-Bernard AE, Cambier J. B cell antigen receptor signaling 101. Mol. Immunol 2004;41:599–613. [PubMed: 15219998]

3. McHeyzer-Williams MG, McHeyzer-Williams LJ, Fanelli Panus J, Bikah G, Pogue-Caley RR, Driver DJ, Eisenbraun MD. Antigen-specific immunity: Th cell-dependent B cell responses. Immunol. Res 2000;22:223–236. [PubMed: 11339358]

4. Mitchison NA. T-cell-B-cell cooperation. Nat. Rev. Immunol 2004;4:308–312. [PubMed: 15057789]

5. Song W, Cho H, Cheng P, Pierce SK. Entry of B cell antigen receptor and antigen into class II peptide-loading compartment is independent of receptor cross-linking. J. Immunol 1995;155:4255–4263. [PubMed: 7594583]

6. Cheng PC, Steele CR, Gu L, Song W, Pierce SK. MHC class II antigen processing in B cells: accelerated intracellular targeting of antigens. J. Immunol 1999;162:7171–7180. [PubMed: 10358163]

7. Pure E, Tardelli L. Tyrosine phosphorylation is required for ligand-induced internalization of the antigen receptor on B lymphocytes. Proc. Natl. Acad. Sci. USA 1992;89:114–117. [PubMed: 1370346]

8. Wagle NM, Kim JH, Pierce SK. Signaling through the B cell antigen receptor regulates discrete steps in the antigen processing pathway. Cell. Immunol 1998;184:1–11. [PubMed: 9626330]

9. Cassard S, Salamero J, Hanau D, Spehner D, Davoust J, Fridman WH, Bonnerot C. A tyrosine-based signal present in Igα mediates B cell receptor constitutive internalization. J. Immunol 1998;160:1767–1773. [PubMed: 9469435]

10. Siemasko K, Eisfelder BJ, Stebbins C, Kabak S, Sant AJ, Song W, Clark MR. Igα and Igβ are required for efficient trafficking to late endosomes and to enhance antigen presentation. J. Immunol 1999;162:6518–6525. [PubMed: 10352267]

11. Siemasko K, Skaggs B, Kabak JS, Williamson E, Brown BK, Song W, Clark MR. Receptor facilitated antigen presentation requires the recruitment of B cell linker protein to Igα. J. Immunol 2002;168:2127–2138. [PubMed: 11859098]

12. Lankar D, Briken V, Adler K, Weiser P, Cassard S, Blank U, Viguier M, Bonnerot C. Syk tyrosine kinase and B cell antigen receptor (BCR) immunoglobulin-α subunit determine BCR-mediated major histocompatibility complex class II-restricted antigen presentation. J. Exp. Med 1998;188:819–831. [PubMed: 9730884]

13. Ma H, Yankee TM, Hu J, Asai DJ, Harrison ML, Geahlen RL. Visualization of Syk-antigen receptor interactions using green fluorescent protein: differential roles for Syk and Lyn in the regulation of receptor capping and internalization. J. Immunol 2001;166:1507–1516. [PubMed: 11160190]

14. Le Roux D, Lankar D, Yuseff MI, Vascotto F, Yokozeki T, Faure-Andre G, Mougneau E, Glaichenhaus N, Manoury B, Bonnerot C, Lennon-Dumenil AM. Syk-dependent actin dynamics regulate endocytic trafficking and processing of antigens internalized through the B-cell receptor. Mol. Biol. Cell 2007;18:3451–3462. [PubMed: 17596518]

15. Stoddart A, Dykstra ML, Brown BK, Song W, Pierce SK, Brodsky FM. Lipid rafts unite signaling cascades with clathrin to regulate BCR internalization. Immunity 2002;17:451–462. [PubMed: 12387739]

16. Braun J, Hochman PS, Unanue ER. Ligand-induced association of surface immunoglobulin with the detergent-insoluble cytoskeletal matrix of the B lymphocyte. J. Immunol 1982;128:1198–1204. [PubMed: 6976988]

17. Park JY, Jongstra-Bilen J. Interactions between membrane IgM and the cytoskeleton involve the cytoplasmic domain of the immunoglobulin receptor. Eur. J. Immunol 1997;27:3001–3009. [PubMed: 9394830]

18. Jugloff LS, Jongstra-Bilen J. Cross-linking of the IgM receptor induces rapid translocation of IgM-associated Igα, Lyn, and Syk tyrosine kinases to the membrane skeleton. J. Immunol 1997;159:1096–1106. [PubMed: 9233602]

19. Melamed I, Downey GP, Aktories K, Roifman CM. Microfilament assembly is required for antigen-receptor-mediated activation of human B lymphocytes. J. Immunol 1991;147:1139–1146. [PubMed: 1907989]

20. Albrecht DL, Mills JW, Noelle RJ. Membrane Ig-cytoskeletal interactions. III. Receptor cross-linking results in the formation of extensive filamentous arrays of vimentin. J. Immunol 1990;144:3251–3256. [PubMed: 2109773]

21. Schreiner GF, Unanue ER. Membrane and cytoplasmic changes in B lymphocytes induced by ligand-surface immunoglobulin interaction. Adv. Immunol 1976;24:37–165. [PubMed: 798475]

22. Schreiner GF, Unanue ER. Capping and the lymphocyte: models for membrane reorganization. J. Immunol 1977;119:1549–1551. [PubMed: 334966]

23. Gabbiani G, Chaponnier C, Zumbe A, Vassalli P. Actin and tubulin co-cap with surface immunoglobulins in mouse B lymphocytes. Nature 1977;269:697–698. [PubMed: 413049]

24. Brown BK, Song W. The actin cytoskeleton is required for the trafficking of the B cell antigen receptor to the late endosomes. Traffic 2001;2:414–427. [PubMed: 11389769]

25. Hao S, August A. Actin depolymerization transduces the strength of B-cell receptor stimulation. Mol. Biol. Cell 2005;16:2275–2284. [PubMed: 15728723]

26. Stoddart A, Jackson AP, Brodsky FM. Plasticity of B cell receptor internalization upon conditional depletion of clathrin. Mol. Biol. Cell 2005;16:2339–2348. [PubMed: 15716350]

27. Vascotto F, Le Roux D, Lankar D, Faure-Andre G, Vargas P, Guermonprez P, Lennon-Dumenil AM. Antigen presentation by B lymphocytes: how receptor signaling directs membrane trafficking. Curr. Opin. Immunol 2007;19:93–98. [PubMed: 17140785]

28. Kessels MM, Engqvist-Goldstein AE, Drubin DG. Association of mouse actin-binding protein 1 (mAbp1/SH3P7), an Src kinase target, with dynamic regions of the cortical actin cytoskeleton in response to Rac1 activation. Mol. Biol. Cell 2000;11:393–412. [PubMed: 10637315]

29. Larbolette O, Wollscheid B, Schweikert J, Nielsen PJ, Wienands J. SH3P7 is a cytoskeleton adapter protein and is coupled to signal transduction from lymphocyte antigen receptors. Mol. Cell. Biol 1999;19:1539–1546. [PubMed: 9891087]

30. Ensenat D, Yao Z, Wang XS, Kori R, Zhou G, Lee SC, Tan TH. A novel *src* homology 3 domain-containing adaptor protein, HIP-55, that interacts with hematopoietic progenitor kinase 1. J. Biol. Chem 1999;274:33945–33950. [PubMed: 10567356]

31. Fenster SD, Kessels MM, Qualmann B, Chung WJ, Nash J, Gundelfinger ED, Garner CC. Interactions between Piccolo and the actin/dynamin-binding protein Abp1 link vesicle endocytosis to presynaptic active zones. J. Biol. Chem 2003;278:20268–20277. [PubMed: 12654920]

32. Qualmann B, Boeckers TM, Jeromin M, Gundelfinger ED, Kessels MM. Linkage of the actin cytoskeleton to the postsynaptic density via direct interactions of Abp1 with the ProSAP/Shank family. J. Neurosci 2004;24:2481–2495. [PubMed: 15014124]

33. Kessels MM, Engqvist-Goldstein AE, Drubin DG, Qualmann B. Mammalian Abp1, a signal-responsive F-actin-binding protein, links the actin cytoskeleton to endocytosis via the GTPase dynamin. J. Cell Biol 2001;153:351–366. [PubMed: 11309416]

34. Drubin DG, Miller KG, Botstein D. Yeast actin-binding proteins: evidence for a role in morphogenesis. J. Cell Biol 1988;107:2551–2561. [PubMed: 3060468]

35. Goode BL, Rodal AA, Barnes G, Drubin DG. Activation of the Arp2/3 complex by the actin filament binding protein Abp1p. J. Cell Biol 2001;153:627–634. [PubMed: 11331312]

36. Pinyol R, Haeckel A, Ritter A, Qualmann B, Kessels MM. Regulation of N-WASP and the Arp2/3 complex by Abp1 controls neuronal morphology. PLoS ONE 2007;2:e400. [PubMed: 17476322]

37. Kaksonen M, Toret CP, Drubin DG. A modular design for the clathrin- and actin-mediated endocytosis machinery. Cell 2005;123:305–320. [PubMed: 16239147]

38. Hinshaw JE. Dynamin and its role in membrane fission. Annu. Rev. Cell. Dev. Biol 2000;16:483–519. [PubMed: 11031245]

39. Connert S, Wienand S, Thiel C, Krikunova M, Glyvuk N, Tsytsyura Y, Hilfiker-Kleiner D, Bartsch JW, Klingauf J, Wienands J. SH3P7/ mAbp1 deficiency leads to tissue and behavioral abnormalities and impaired vesicle transport. EMBO J 2006;25:1611–1622. [PubMed: 16601697]

40. Mise-Omata S, Montagne B, Deckert M, Wienands J, Acuto O. Mammalian actin binding protein 1 is essential for endocytosis but not lamellipodia formation: functional analysis by RNA interference. Biochem. Biophys. Res. Commun 2003;301:704–710. [PubMed: 12565838]

41. Han J, Kori R, Shui JW, Chen YR, Yao Z, Tan TH. The SH3 domain-containing adaptor HIP-55 mediates c-Jun N-terminal kinase activation in T cell receptor signaling. J. Biol. Chem 2003;278:52195–52202. [PubMed: 14557276]

42. Le Bras S, Foucault I, Foussat A, Brignone C, Acuto O, Deckert M. Recruitment of the actin-binding protein HIP-55 to the immunological synapse regulates T cell receptor signaling and endocytosis. J. Biol. Chem 2004;279:15550–15560. [PubMed: 14729663]

43. Han J, Shui JW, Zhang X, Zheng B, Han S, Tan TH. HIP-55 is important for T-cell proliferation, cytokine production, and immune responses. Mol. Cell. Biol 2005;25:6869–6878. [PubMed: 16055701]

44. Germain RN, Jenkins MK. In vivo antigen presentation. Curr. Opin. Immunol 2004;16:120–125. [PubMed: 14734120]

45. Murphy DB, Rath S, Pizzo E, Rudensky AY, George A, Larson JK, Janeway CA Jr. Monoclonal antibody detection of a major self peptide: MHC class II complex. J. Immunol 1992;148:3483–3491. [PubMed: 1375245]

46. Lerner EA, Matis LA, Janeway CA Jr, Jones PP, Schwartz RH, Murphy DB. Monoclonal antibody against an Ir gene product? J. Exp. Med 1980;152:1085–1101. [PubMed: 6158546]

47. Lila T, Drubin DG. Evidence for physical and functional interactions among two *Saccharomyces cerevisiae* SH3 domain proteins, an adenylyl cyclase-associated protein and the actin cytoskeleton. Mol. Biol. Cell 1997;8:367–385. [PubMed: 9190214]

48. Dawson JC, Legg JA, Machesky LM. Bar domain proteins: a role in tubulation, scission and actin assembly in clathrin-mediated endocytosis. Trends Cell Biol 2006;16:493–498. [PubMed: 16949824]
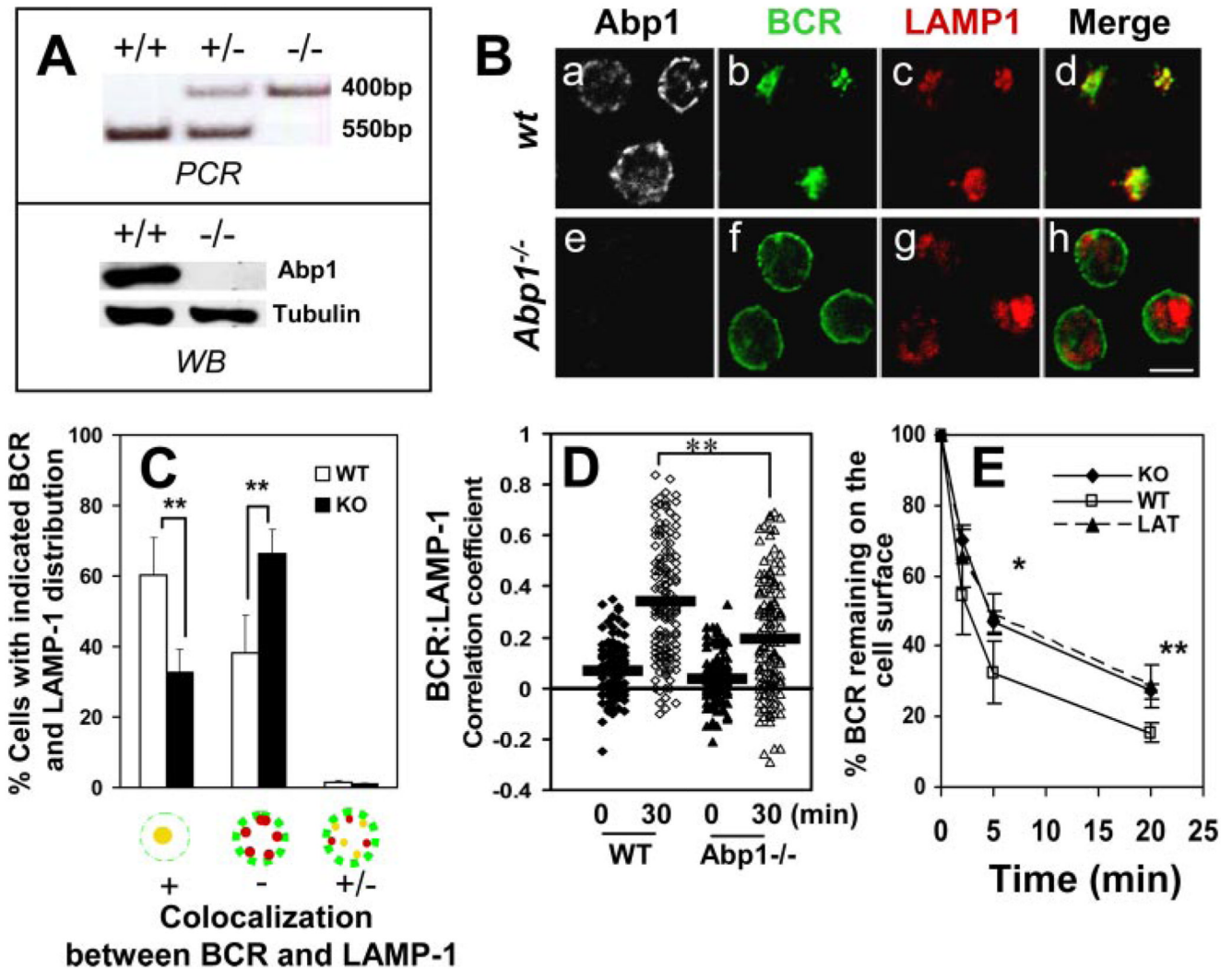
FIGURE 1.
Abp1 gene knockout reduces the rates of BCR internalization and movement from the plasma membrane to late endosomes. *A*, Abp1 gene knockout in mice was confirmed using PCR (*top panel*) and Western blot (*bottom panel*). *B*, Splenic B cells from wt and Abp1$^{-/-}$ mice were incubated with AF488-F(ab′)$_2$ goat anti-mouse IgM at 4°C for labeling and cross-linking the surface BCR and then chased at 37°C for 30 min. Cells were fixed, permeabilized, and labeled with anti-Abp1, anti-LAMP-1, and fluorochrome-conjugated secondary Abs. Cells were analyzed using a confocal fluorescence microscope. Shown are representative images of three independent experiments. Bar, 5 μm. *C*, Cells were categorized by visual inspection into three different categories, as follows: cells showing extensive colocalization, no colocalization, and partial colocalization between the BCR and LAMP-1. Cells from more than 10 randomly selected fields containing at least 15 cells per field from three independent experiments were inspected. Shown are the average percentages (±SD) of cells in each of the three categories. **, $p < 0.01$. *D*, Shown are correlation coefficients between the staining of the BCR and LAMP-1 in ~100 individual cells of three independent experiments. ▬, Represent mean correlation coefficients. **, $p < 0.0001$. *E*, The surface BCR was labeled with biotin-F(ab′)$_2$ goat anti-mouse IgM at 4°C and chased at 37°C for indicated times. Biotin-anti-mouse IgM left on the surface after the

chase was detected by PE-streptavidin and quantified using a FACSCalibur. For latrunculin (LAT) treatment, cells were incubated with 5 μM latrunculin before and during the analysis. The data were plotted as the percentages of the surface-labeled BCR at time 0. Shown are the averages (±SD) of three independent experiments. *, $p < 0.05$; **, $p < 0.01$.
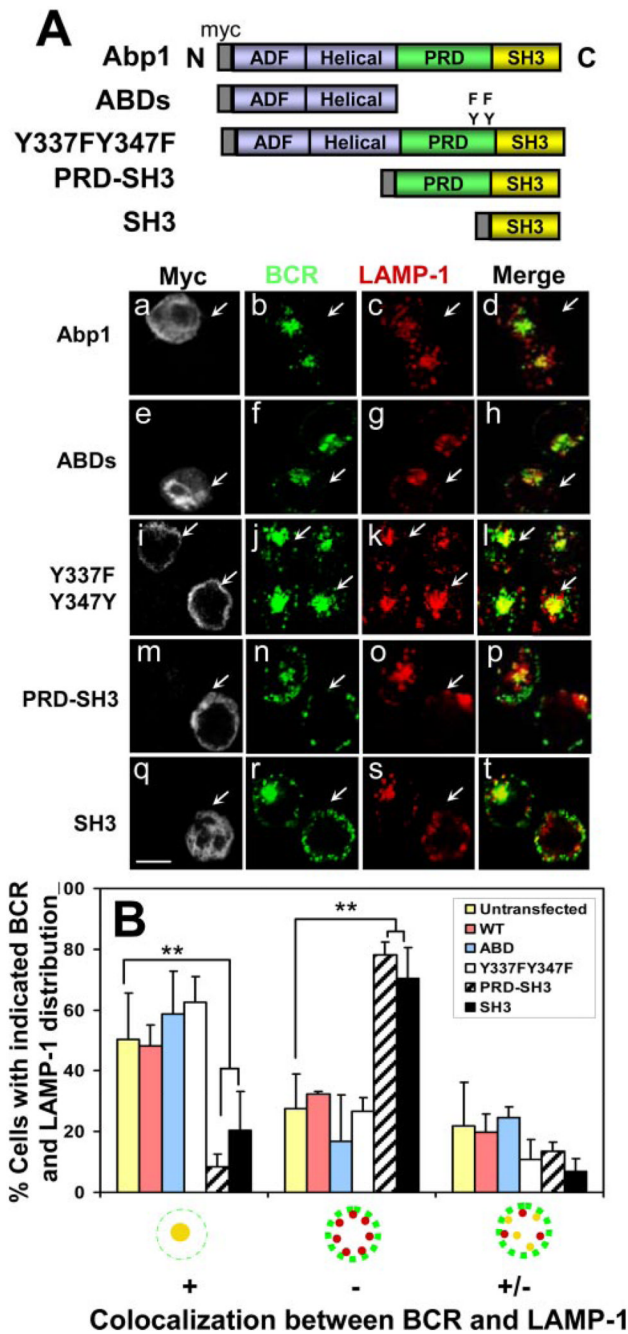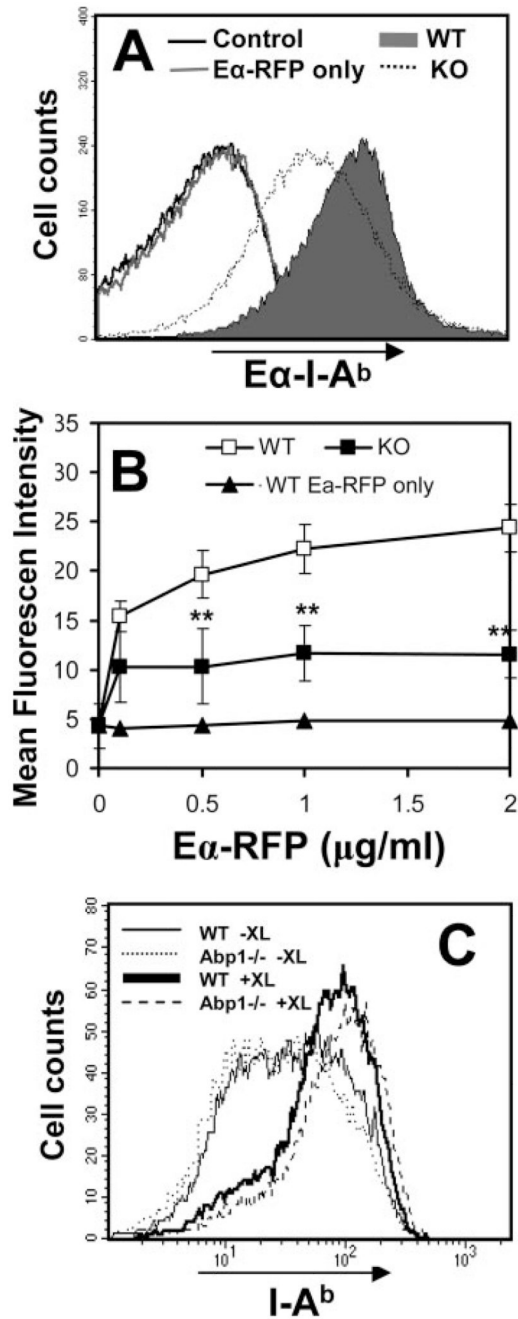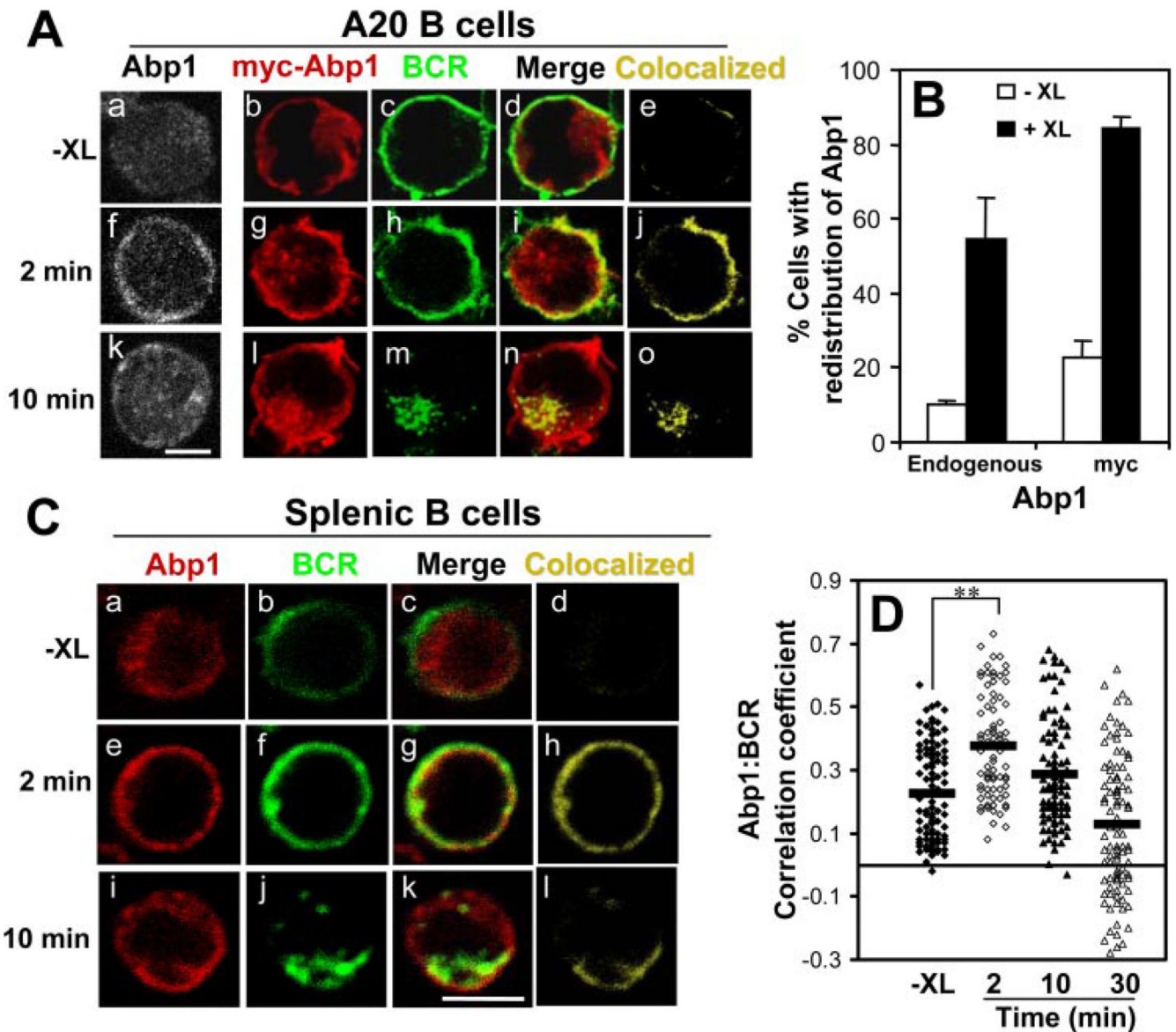
FIGURE 2.
The effect of overexpression of Abp1 domains and mutants on the movement of the BCR from the cell surface to late endosomes. *A*, B cell lymphoma A20 cells were transiently transfected with *myc*-tagged full-length protein of Abp1 (Abp1), Abp1 with its two tyrosine phosphorylation sites mutated (Y337FY347F), ABDs, and PRD and/or SH3 domains (PRD-SH3 and SH3) of Abp1. Twenty-four hours after transfection, cells were labeled with AF488 goat anti-mouse IgG for 20 min at 4°C and chased for 30 min at 37°C. Cells were fixed, permeabilized, and labeled with anti-*myc* Ab for *myc*-Abp1 and anti-LAMP-1 mAb for late endosomes. Arrows indicate cells expressing transfected proteins. Bar, 10 µm. *B*, Cells were categorized by visual inspection into three different categories, as described in Fig. 1.

Shown are the average percentages (±SD) of cells in each of the three categories from three independent experiments. **, $p < 0.01$.
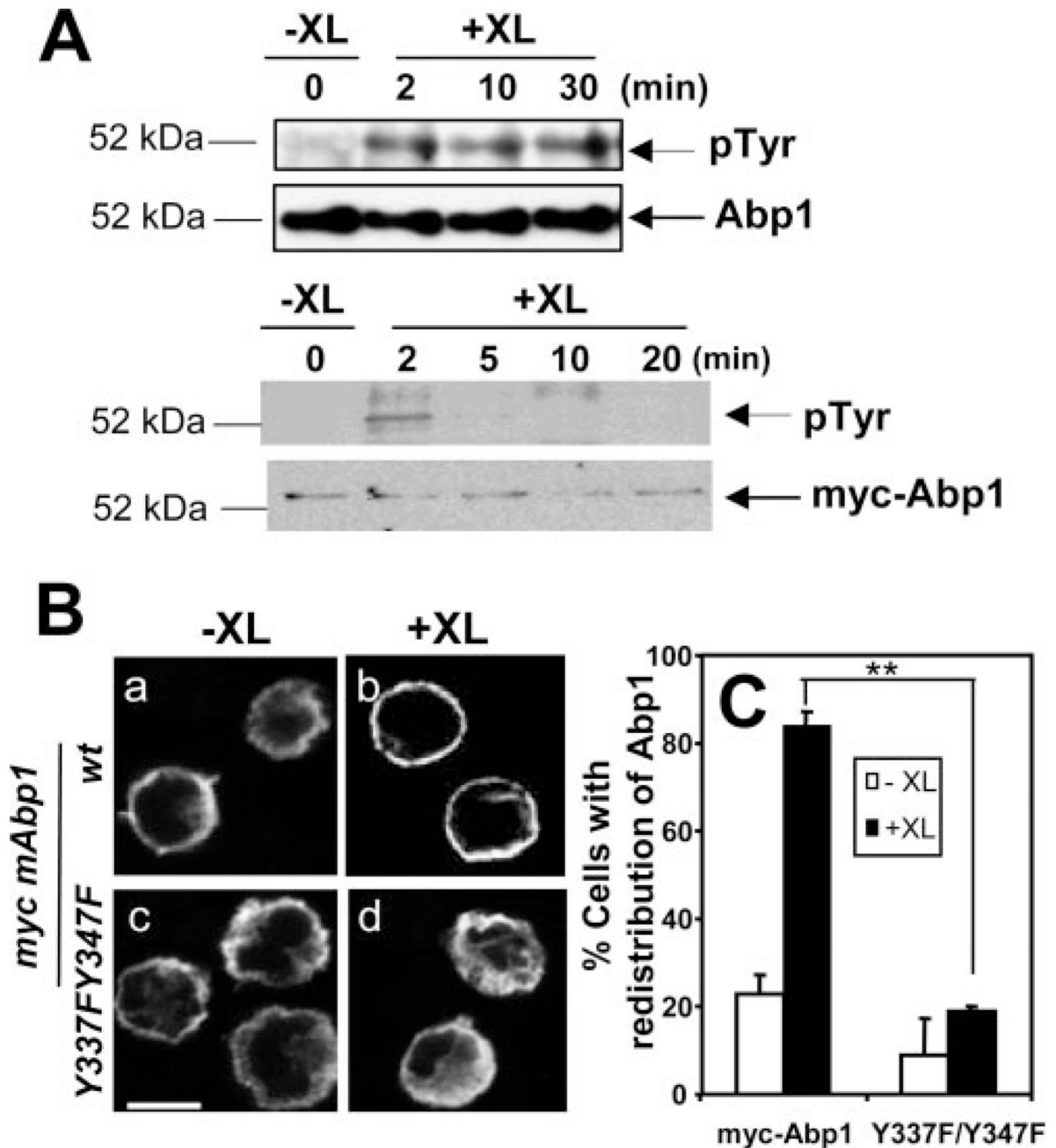
FIGURE 3.
B cells from Abp1 knockout mice are defective in Ag processing and presentation. *A*, Splenic B cells from wt (filled) and Abp1$^{-/-}$ (dotted) mice were incubated at 37°C for 10 min with EαRFP (1 µg/ml) alone (gray line) or with the Ab complex that targets EαRFP to the BCR. Cells were washed and incubated at 37°C for 14 h. Eα peptide-loaded MHC class II I-A^b complexes on the cell surface were detected using anti-Y-Ae mAb and quantified using flow cytometry. *B*, Splenic B cells from wt (□) and Abp1$^{-/-}$ (■) mice were incubated with different concentrations of EαRFP alone or EαRFP-Ab complexes, as described in *A*. Splenic B cells from wt mice were incubated with different concentrations of EαRFP alone (▲). Cells were stained and analyzed, as described above. Shown are the averages (±SD) of

mean fluorescence intensity of Y-Ae staining from three independent experiments. **, $p <$ 0.01. *C*, The expression levels of MHC class II I-A^b of splenic B cells from wt (solid lines) and Abp1$^{-/-}$ (dotted lines) mice before ($-$XL) and after ($+$XL) exposure to EαRFP-Ab complexes were measured using flow cytometry.
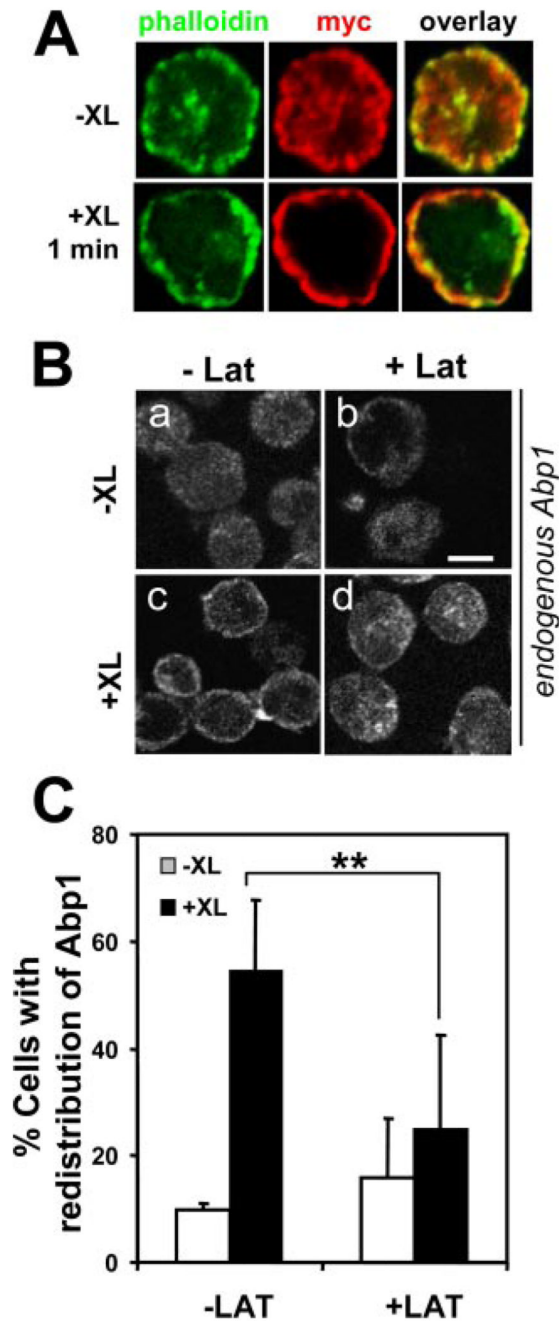
FIGURE 4.
BCR activation induces the redistribution of Abp1 to the plasma membrane. *A* and *C*, A20 (*A*) and splenic B cells (*C*) were treated (+XL) or untreated (−XL) with either goat anti-mouse IgG (*A, a, f*, and *k*) or AF488 goat anti-mouse IgG + M (*A, b–e, g–j*, and *l–o*, and *C*) at 4°C and chased at 37°C for indicated times. After fixation and permeabilization, cells were labeled with anti-Abp1 Ab for the endogenously expressed Abp1 (*A, a, f*, and *k*, and *C*) or anti-*myc* Ab for *myc*-Abp1 (*A, b–e, g–j*, and *l–o*). Cells were analyzed using a confocal fluorescence microscope. Shown are representative images from three independent experiments. Bar, 5 µm. *B*, The redistribution of endogenous Abp1 and *myc*-Abp1 from the cytoplasm to the cell surface after BCR cross-linking for 2 min was quantified by visual inspection. Over 100 cells from five randomly selected fields of each experiment were analyzed, and the numbers of cells showing Abp1 concentrated on the cell surface were plotted as percentages of the total number of cells inspected. Shown are averages (±SD) from three independent experiments. *D*, The correlation coefficients of endogenous Abp1 with the BCR in splenic B cells before and after BCR cross-linking was determined using

the LSM510 software. Shown are the data generated from >100 cells of two independent experiments. ▬, Indicate the mean. **, $p < 0.0001$.

FIGURE 5.
BCR-induced cellular redistribution of Abp1 is dependent on BCR-induced tyrosine phosphorylation of Abp1. *A*, Untransfected A20 B cells (*top*) and A20 B cells transfected with *myc*-Abp1 (*bottom*) were treated (+XL) or untreated (−XL) with goat anti-mouse IgG for varying lengths of time to activate the BCR. Then cells were lysed, and endogenous Abp1 and *myc*-Abp1 were purified from cell lysates by immunoprecipitation using anti-Abp1 and anti-*myc* Abs, respectively. The immunoprecipitates were analyzed by SDS-PAGE and Western blot, probing with anti-phosphotyrosine mAb (4G10). The blots were stripped and reblotted with anti-Abp1 or anti-*myc* Ab. Shown are representative blots of three independent experiments. *B*, A20 cells transiently transfected with wt *myc*-Abp1 (*Ba-*

Bb) and *myc*-Abp1 Y337F/Y347F (*Bc-Bd*) were treated (+XL) and untreated (−XL) with goat anti-mouse IgG for 2 min, and then fixed, permeabilized, and labeled with Cy3 anti-*myc* mAb for *myc*-Abp1. Cells were analyzed using a confocal fluorescence microscope. Shown are representative images of three independent experiments. Bar, 10 µm. *C*, Cells in images were quantified, as described in Fig. 4*B*. Over 100 cells from three independent experiments were analyzed. Shown are the averages (±SE) from three independent experiments. **, $p < 0.01$.

FIGURE 6.
BCR-induced Abp1 redistribution depends on the actin cytoskeleton. *A*, A20 cells transiently transected with *myc*-Abp1 were incubated with (+XL) or without (−XL) goat anti-mouse IgG for 1 min. After fixation and permeabilization, cells were labeled with AF488-phalloidin for F-actin and Cy3 anti-*myc* mAb for *myc*-Abp1. *B*, A20 cells were pretreated with or without latrunculin (Lat) and activated in the presence or absence of Lat for 1 min. Cells were labeled with anti-Abp1 Ab and AF488-conjugated secondary Ab and analyzed using a confocal fluorescence microscope. Shown are representative images of three independent experiments. Bar, 5 µm. *C*, Cells in images quantified as described in Fig. 4*B*, and shown are averages (±SD) from three independent experiments. **, $p < 0.01$.
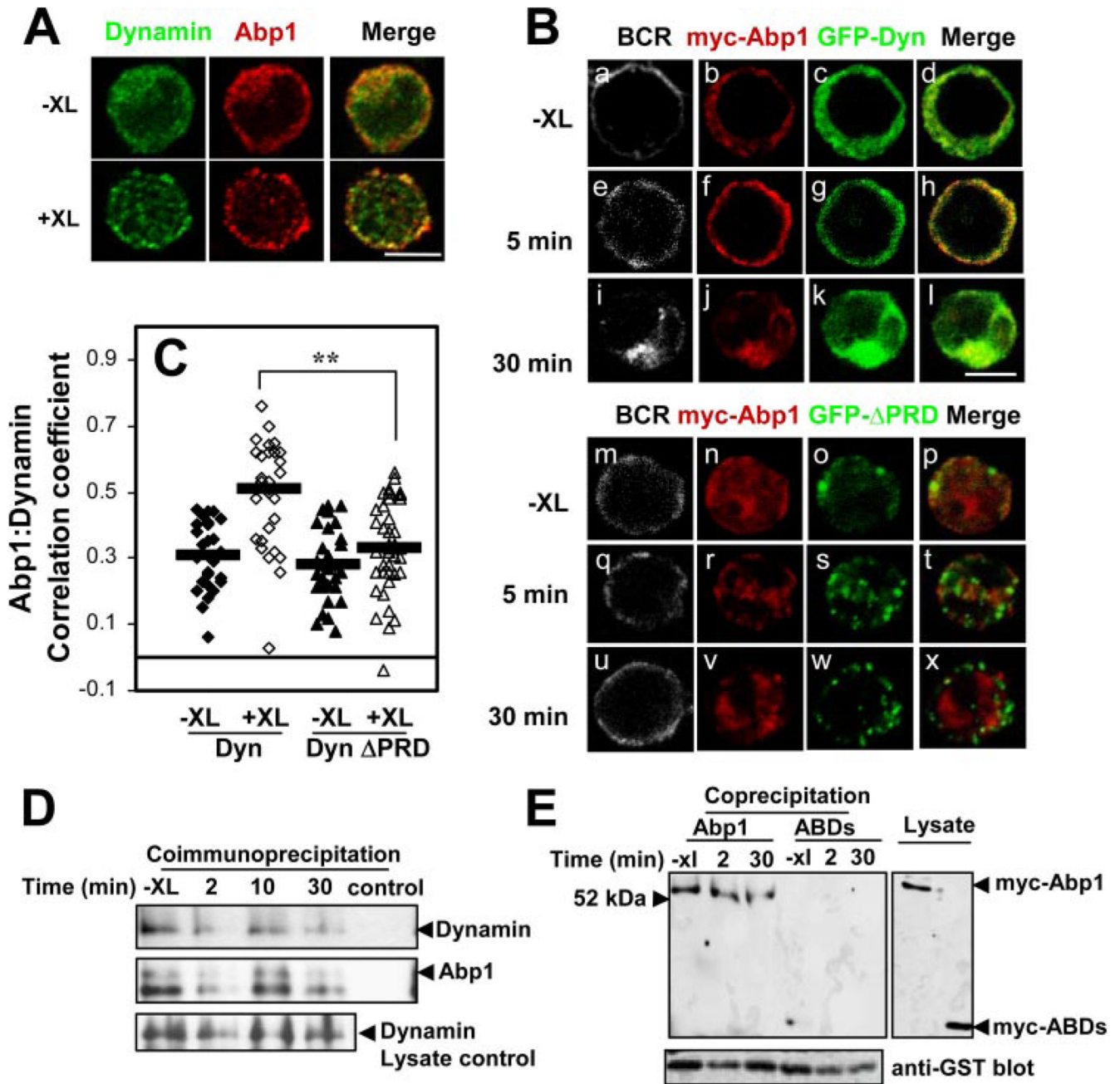
FIGURE 7.
Interaction of Abp1 with dynamin 2. *A*, A20 cells were incubated with (+XL) and without (−XL) goat anti-mouse IgG for 2 min and then fixed, permeabilized, and labeled with anti-Abp1 and anti-dynamin 2 Abs and corresponding secondary Abs. The cells were cotransfected using a confocal fluorescence microscope. Shown are representative images from three independent experiments. Bar, 5 µm. *B*, A20 cells were cotransfected with *myc*-Abp1 and GFP-dynamin 2 (GFP-Dyn) (*a–l*) or GFP-dynamin 2 with PRD deletion (GFP-ΔPRD) (*m–x*). The cells were incubated with (*e–l, q–x*) and without (−XL) (*a–d, m–p*) goat anti-mouse IgG for indicated times, and then fixed, permeabilized, and labeled with Cy3 anti-*myc* Ab to label *myc*-Abp1. The cells were analyzed by confocal fluorescence

microscopy. Shown are representative images from three independent experiments. Bar, 5 µm. *C*, Shown are the correlation coefficients between *myc*-Abp1 and GFP-Dyn or GFP-ΔPRD in the cell surface area of >30 cells from three independent experiments. ▬▬, Represent the mean correlation coefficient. **, $p < 0.00001$. *D*, A20 cells were treated or untreated (−XL) with BCR cross-linking Ab for indicated times. The cells were lysed, and the cell lysates were subjected to immunoprecipitation using goat anti-Abp1 Ab. The cell lysates and immunoprecipitates were analyzed using SDS-PAGE and Western blot, probing for dynamin 2. The blots were stripped and reblotted with anti-Abp1 Ab as loading controls. Shown are representative blots from three independent experiments. *E*, A20 cells transiently transfected with *myc*-Abp1 or *myc*-Abp1 ABDs were activated by cross-linking the BCR with goat anti-mouse IgG for indicated times and then lysed. The cell lysates were incubated with GST-fusion of dynamin PRD-bound beads. The cell lysates and precipitates were subjected to SDS-PAGE and Western blot, probing for *myc*-Abp1. The blots were stripped and reblotted with anti-GST Ab. Shown are representative blots from two independent experiments.